Growth of Single-Walled Carbon Nanotubes by the Rapid Heating of a Supported Catalyst

ARTICLE *in* CHEMISTRY OF MATERIALS · NOVEMBER 2004

Impact Factor: 8.35 · DOI: 10.1021/cm0495111

6 AUTHORS, INCLUDING:

Ian Kinloch
The University of Manchester
131 PUBLICATIONS **7,300** CITATIONS
SEE PROFILE

Charanjeet Singh
University of Cambridge
12 PUBLICATIONS **986** CITATIONS
SEE PROFILE

Growth of Single-Walled Carbon Nanotubes by the Rapid Heating of a Supported Catalyst

Ya-Li Li,[†] Ian A. Kinloch,[†] Milo S. P. Shaffer,[†,‡] Charanjeet Singh,[†,§] Junfeng Geng,[∥] Brian F. G. Johnson,[∥] and Alan H. Windle*,[†]

Department of Materials Science and Metallurgy, University of Cambridge, Pembroke Street, Cambridge CB2 3QZ, and Department of Chemistry, University of Cambridge, Lensfield Road, Cambridge CB2 1EW, U.K.

Received March 22, 2004. Revised Manuscript Received September 15, 2004

Single-walled carbon nanotubes (SWNTs) have been synthesized by the rapid injection of a nickel formate/silica gel catalyst/support into a hot fluidized-bed reactor. The initial rapid heating of the catalyst in the hydrocarbon feedstock was found to be essential for the nucleation of SWNTs since only amorphous or graphitic carbon particles were formed without it. These results suggest that the rapid heating of the catalyst precursor enables the formation of the small metal particles required for SWNT growth, probably due to the accelerated thermal decomposition of the catalyst precursor and enhanced nucleation rate. The growth of the SWNTs was investigated by the adoption of different methods for introducing the catalyst, and by varying the synthesis parameters including the catalyst loading, hydrocarbon gas flow rate, and concentration. The results found that SWNTs formed only under certain reaction conditions. The nanotubes produced were characterized by electron microscopy and Raman spectroscopy.

1. Introduction

The catalytic chemical vapor decomposition process (CCVD) has proved to be a feasible production route for carbon nanotubes, as demonstrated by the successful synthesis of multiwalled carbon nanotubes (MWNTs) in the form of both random aggregates and well-ordered films.[1−3] The extension of the process to the synthesis of single-walled carbon nanotubes (SWNTs), which are preferred to MWNTs for some applications because of their superior electrical and mechanical properties,[2,3] is a current objective. In recent years, numerous studies have been made of different catalysts and precursors based upon Fe, Co, and Ni compounds supported on various substrates such as SiO_2, MgO and Al_2O_3. Typically, either the catalysts are physically impregnated onto the substrate or both the catalyst and the substrate are formed by a sol−gel process.[4−14] These studies showed that the growth of SWNTs is more difficult to control than that of MWNTs.

SWNT synthesis has been reported to be affected by many conditions, including the combination of the catalyst and support used, the metal loadings on the supports,[4−6,9−11] their preheat treatment,[6] the hydrocarbon gas flow rate and its concentration,[12] the reaction temperature,[9,11,12] and the chemical properties of the carbon feedstock.[14] In particular, the physical and chemical properties of the catalyst/support are found to be important to the growth of SWNTs, since some systems show quite a wide synthesis window for SWNT production, while many others yield only MWNTs or amorphous carbon regardless of the synthesis conditions.

Currently, the detailed mechanism for SWNT growth is unclear. However, it is generally agreed that the presence of the small catalyst particles similar in diameter to SWNTs (less than a few nanometers) is necessary for the nucleation of SWNTs and their subsequent growth under suitable reaction conditions. The control of the formation of such small diameter catalyst particles and their stabilization at high growth

* To whom correspondence should be addressed. Phone: (0044)-1223-334321. Fax: (0044)-1223-334366. E-mail: ahw1@cam.ac.uk.
† Department of Materials Science and Metallurgy.
‡ Present address: Department of Chemistry, Imperial College Science Technology & Medicine, Imperial College Rd., London SW7 2AZ, U.K.
§ Present address: Thomas Swan and Co. Ltd., Consett, County Durham, U.K.
∥ Department of Chemistry.

(1) Andrews, R.; Jacques, D.; Qian, D.; Rantell, T. *Acc. Chem. Res.* **2002**, *35*, 1008.
(2) Baughman, R. H.; Zakhidov, A. A.; Heer, W. A. *Science* **2002**, *297*, 787.
(3) Ajayan, P. M. *Chem. Rev.* **1999**, *99*, 1787.
(4) Kong, J.; Cassel, A. M.; Dai, H. J. *Chem. Phys. Lett*. **1998**, *292*, 567.
(5) Colomer, J. F.; Stephan, C.; Lefrant, S.; Tendeloo, G. Van; Willems, I.; Konya, Z.; Fonseca, A.; Laurent, Ch.; Nagy, J. B. *Chem. Phys. Lett.* **2000**, *317*, 83.
(6) Flahaut, E.; Govindaraj, A.; Peigney, A.; Laurent, C.; Rousset, A.; Rao, C. N. R. *Chem. Phys. Lett.* **1999**, *300*, 236.
(7) Maruyama, S.; Kojima, R.; Miyauchi, Y.; Chiashi, S.; Kohno, M. *Chem. Phys. Lett*. **2002**, *360*, 229.
(8) Su, M.; Zheng, B.; Liu, J. *Chem. Phys. Lett.* **2000**, *322,* 321.
(9) Alvarez, W. E.; Pompeo, F.; Herrera, J. E.; Balzano, L.; Ressco, D. E. *Chem. Mater.* **2002**, *14*, 1853.
(10) Tang, S.; Zhong, Z.; Xiong, Z.; Sun, L.; Liu, L.; Lin, J.; Shen, Z. X.; Tan, K. L. *Chem. Phys. Lett.* **2001**, *350*, 19.
(11) Kitiyanan, B.; Alvarez, W. E.; Harwell, J. H.; Resasco, D. E. *Chem. Phys. Lett.* **2000**, *317*, 497.
(12) Zheng, B.; Li, Y.; Liu, J. *Appl. Phys.* **2002**, *A74*, 345.
(13) Geng, J.; Singh, C.; Shephard, D. S.; Shaffer, M. S. P.; Johnson, B. F. G.; Windle, A. H. *Chem. Commun.* **2002**, 2666.
(14) Rao, C. N. R. *Mater. Res. Innovations* **1998**, *2*, 128.

10.1021/cm0495111 CCC: $27.50
Published on Web 11/20/2004

temperatures is seen as an important criterion in the production of SWNTs.

Previously, the processes to create active catalyst particles for SWNTs were mainly directed toward the chemical routes, including forming a solid solution of the catalyst and substrate, chemically etching the substrate or solid solution, or using different systems of catalysts and substrates. Since the catalyst particles are formed by the thermal decomposition of the precursor on the surface of the substrate, the properties of the catalyst particles formed are not only determined by the physical and chemical properties of the catalyst and the support materials but also affected by its decomposition process. The majority of the work conducted on the growth of nanotubes from supported catalysts has used a "fixed (catalyst) bed", whereby the supported catalyst is packed into a furnace followed by heating it to the synthesis temperature and then passing a hydrocarbon gas over the bed. The rate of heating of the supported catalyst in this process is usually low, and the decomposition of the catalyst precursors occurs during the ramping of the furnace to the reaction temperature. This slow heating of the catalyst and hence long annealing time of the metal particles on the substrates can readily cause the formation of larger catalyst particles through ripening, especially when there is a weak chemical interaction between the catalyst and support. Therefore, a rapid heating and decomposition process could aid the generation of the small metallic particles by minimizing the sintering time, thus providing active catalysts for SWNT growth.

In the present work, we have been able to show that the rapid addition of a supported catalyst into a hot fluidized bed reactor can activate a catalyst/support system which is inert in fixed-bed conditions and thus enable the growth of SWNTs in a controlled manner. This affect was demonstrated by using nickel formate as the catalyst precursor impregnated onto silica gel particles. While this catalyst/support yielded only amorphous carbon and a few MWNTs when using the fixed-bed synthesis, we have found that SWNTs can be produced reproducibly by simply applying an additional heating procedure as the supported catalyst is fed into the reactor. The synthesis was conducted via the injection of the supported catalyst into a fluidized-bed reactor at the synthesis temperature, followed by fluidizing the catalyst particles by a gas flow of a hydrocarbon feedstock. For comparison, experiments in which the catalyst precursor was cold-loaded into the reactor prior to heating were also conducted. By these means, we were able to evaluate the effects of the rapid heating of the catalyst. The effects of nickel loading on the support and the synthesis conditions on the growth of carbon products were investigated. The products were characterized by electron microscopy and Raman spectroscopy.

2. Experimental Section

The reactions were conducted using a fluidized-bed reactor which consisted of two concentric quartz tubes, with the inner one (i.d. 20 mm and 1000 mm long) sealed in the middle with a porous silica disk that supported the catalyst bed during fluidization (Figure 1). The outer, larger diameter tube (i.d. 60 mm and 1400 mm long) enclosed the fluidized-bed tube such that the apparatus was gastight. At the top of the reactor, a

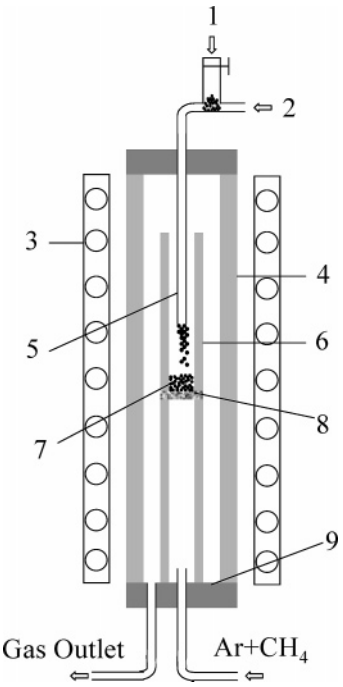

Figure 1. A schematic diagram of the fluidized-bed reactor used for the growth of SWNTs: (1) powder feeder, (2) carrier gas inlet, (3) tube furnace, (4) outer quartz tube, (5) powder injection inlet, (6) inner quartz tube, (7) fluidized bed, (8) porous silica support, (9) base of reactor.

powder feeder was connected to an inlet tube (i.d. 6 mm) going down into the fluidized-bed tube. The catalyst/support powders were placed in the feeder and were fed from the top of the reactor onto the bed using an argon gas flow.

The catalyst/support used consisted of nickel formate (Degussa Chemical Ltd.) and silica gel (Merck Chemical Ltd., silica gel 60, 50 μm mean diameter, 500 m^2/g surface area, and 0.79 cm^3/g pore volume). The catalyst/support was prepared by dispersing silica in an aqueous nickel formate solution (1.6×10^{-2} M) and stirring for 30 min at room temperature, followed by drying at 70 °C for 25 h, and then at 90 °C for 42 h. The dried catalyst was ground gently to break up the loose agglomerates of the particles that could have formed during drying. In this way, catalysts with different nickel loadings (0.7, 1.5, 2.3, 3.0, 5.0, 10, 20, and 30 wt %) were prepared.

For the synthesis, the furnace was heated to the reaction temperature (860 °C) at a rate of 25 °C/min in argon. A 100−500 mg sample of the nickel formate/silica gel catalyst was then fed into the fluidized bed by a carrier gas, with the carrier gas being either pure argon or a mixture of methane and argon (typically $CH_4/Ar = 1$ at a flow rate of 1200 mL/min). In the case of using pure argon as the carrier gas (600 mL/min), methane was also passed upward through the fluidized bed at the same flow rate to provide an immediate carbon source for the nickel particles that formed. After the catalysts had been fed in, the carrier flow was stopped and replaced by the up-flow of methane and argon in fixed proportions ranging from $CH_4/Ar = 1$ to $CH_4/Ar = 3$, with the combined flow rate being set in the range of 0.5−2.4 L/min. The syntheses were conducted at atmospheric pressure, and the typical reaction time was 20 min.

The carbon products were characterized by micro Raman spectrometry (Ar^+ laser incident, $\lambda = 514.5$ nm, 25 mW), scanning electronic microscopy (SEM), and transmission electronic microscopy (TEM; JEOL-200CX, 200kV). The samples for the Raman analysis and SEM were prepared by simply placing the as-produced powders onto a glass slide and a conductive metal support respectively. The samples for the TEM observation were prepared by dispersing the product

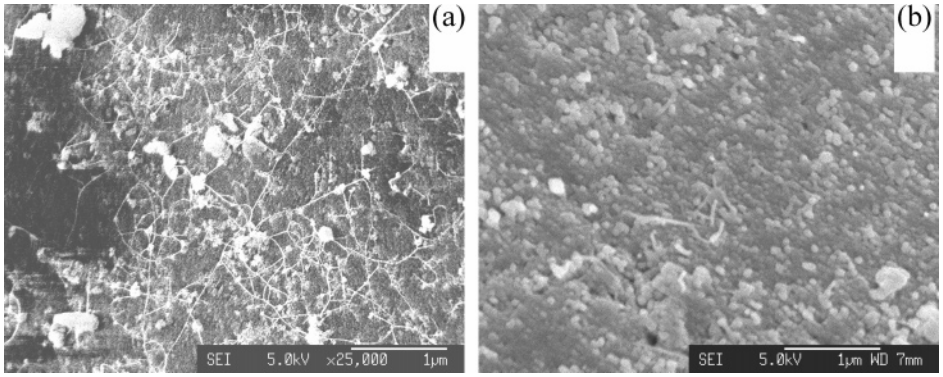

Figure 2. SEM images of the products synthesized by (a) the hot-injection regime and (b) cold-loading of catalysts in the fluidized-bed reactor using nickel formate/silica gel catalyst/support. The images show the presence of nanotubes on the surfaces of the silica gel particles after the hot-injection synthesis (a) but not after the cold-loading synthesis (b). The synthesis conditions were a catalyst nickel loading of 3.5 wt %, synthesis temperature of 860 °C, and $CH_4/Ar = 1$.

powders in ethanol assisted by ultrasonication and then dropping the dispersion onto a carbon-coated copper grid.

3. Results and Discussion

3.1. Synthesis. The experimental setup allowed the syntheses to be carried out with two different methods of heating the catalyst: (i) heating the catalyst/support rapidly by injecting it from the powder feeder directly into the hot bed at the synthesis temperature, immediately followed by fluidization synthesis, and (ii) placing the catalysts onto the bed at room temperature and then heating the bed with the furnace as it is ramped to the synthesis temperature, a protocol typical of fixed-bed synthesis. Synthesis was conducted with each method using otherwise identical catalyst and reaction conditions, so that the effect of the initial catalyst heating rate was isolated. Results showed that SWNTs could be produced only when the catalysts were injected into the preheated furnace (method i). Figure 2a shows the formation of fibrous materials on the surfaces of the silica gel particles obtained by the injection of 3.5 wt % nickel loaded catalysts into the fluidized bed at 860 °C using a carrier gas consisting of methane and argon (1.2 mL/min, $CH_4/Ar = 1$). Raman analysis of this product showed the presence of SWNTs, as characterized by the structure within the strong G band at 1593 cm^{-1} and the radial breath modes (RBMs) in the low-frequency range (100−300 cm^{-1}) (Figure 3). In comparison, the synthesis conducted by cold-loading of the catalyst produced only amorphous carbon products. SEM observation (Figure 2b) showed that the surfaces of the silica gel particles, although blackened by carbon deposit, had no evidence of any fibrous material. Raman analysis gave a spectrum displaying two broad bands, at 1345 and 1576 cm^{-1}, known as the D and G bands, respectively, which are characteristic of graphitic carbon, but none of the features which would suggest SWNTs were present (Figure 3).

There are two aspects in which care has to be taken in interpreting the SEM and Raman evidence for SWNTs. First, the FEGSEM instrument used does not have sufficient resolution to see individual nanotubes. However, the fibrous elements seen, which branch extensively (see Figures 4 and 5), consist of bundles of perhaps several hundred SWNTs, which split and reconnect. Such a bundle structure is very characteristic of SWNT material. Figure 4 shows a high-resolution

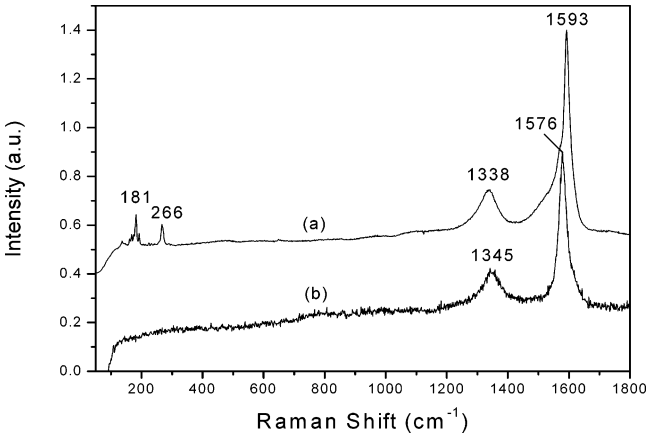

Figure 3. A comparison of the Raman spectrum obtained from the carbon products synthesized by (a) the hot-injection process and (b) cold-loading of catalysts. The samples were the same as those shown in the micrographs in Figure 2.

TEM micrograph of these bundles showing the individual single-walled tubes and branching of the bundles themselves. The scanning micrographs are also useful in demonstrating the absence of MWNTs and other forms of carbon for synthesis under optimum conditions. The RBM peaks of the Raman spectrum are fingerprints of single-walled nanotubes. However, these are resonant phenomena, and their intensity is not, by itself, a reliable guide to the concentration of the SWNTs. The resonance aspects of the RBMs also mean that there are SWNTs of particular diameters which do not show upon any peak.

The growth of SWNTs under the hot-injection condition suggests that a rapid exposure to heat of the catalyst precursor assists in the formation of SWNTs. The formation of the small active catalyst particles in this case could be attributed to the accelerated thermal decomposition of nickel formate on the surfaces of the support due to the rapid exposure of the catalyst precursor to the high temperatures. Nucleation and growth of SWNTs occurred under such conditions immediately on the active metal catalyst particles before ripening through sintering could occur. (We suggest that, once a metal particle has nucleated a nanotube, further sintering is repressed.) It appears that a certain heating rate is needed to achieve such small nickel particles which are active for SWNT growth. During hot injection, the catalyst/support particles were heated

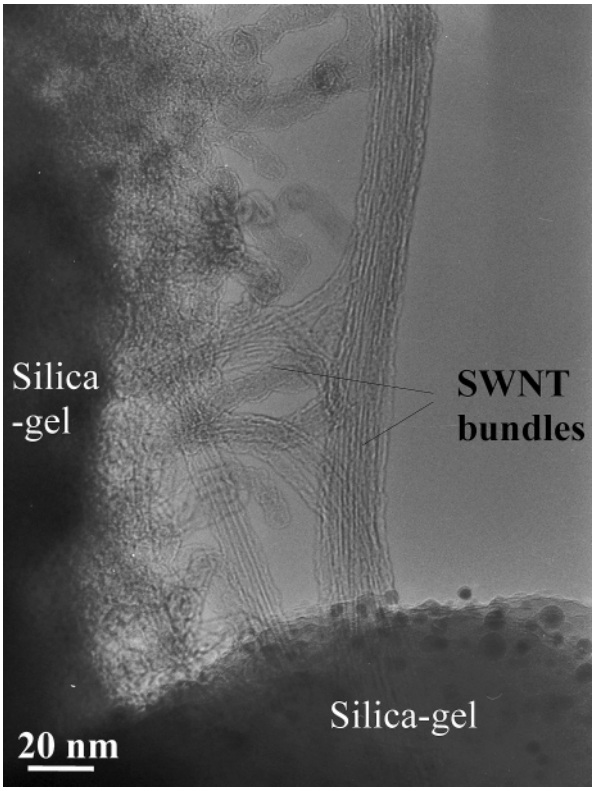

Figure 4. TEM images of the SWNTs grown using 2.3 wt % nickel loaded catalysts at $CH_4/Ar = 1$ and 860 °C. Bundles of SWNTs can be seen spanning across the silica gel particles' surfaces.

from room temperature at the top of the reactor to the synthesis temperature of 860 °C in the furnace within the typical heating distance of ~200 mm. The heating rate under the typical injection condition of 600 mL/min of carrier gas is estimated to be $\sim 4.5 \times 10^3$ °C/s. A fast heating rate could also be reached by simply dropping the catalyst from the top of the reactor by gravity, in which case it was estimated as $\sim 1.8 \times 10^3$ °C/s. Experiments conducted in the absence of a carrier gas flow, where the catalyst/support particles fell under gravity, also generated SWNTs. The effects of lower heating rates were investigated using a horizontal furnace. Here the catalyst/support particles were placed in a ceramic boat and pushed from a cold end of the reactor into the hot zone to give a heating rate of ~25 °C/s. It was found that only a few multiwalled and no single-walled nanotubes were produced under such slow heating conditions. The effects of the heating rate on the growth of carbon nanotubes were also studied using fumed silica substrates, where some SWNTs were apparent under slow heating conditions, but the density of the SWNTs increased with the increasing heating rate. Also, the fumed silica supported catalyst was capable of producing SWNTs even when held at the high reaction temperatures for periods for up to 45 min prior to reaction, showing the stability of the catalyst particles. These results suggest that the requirement of the heating rate for SWNT nucleation changed with the nature of the substrates, with the fumed silica having a rougher surface area than silica gel particles which apparently hinder the surface wetability and therefore sintering of the nanosize particles (see ref 13).

The synthesis of carbon nanotubes in fluidized-bed reactors has been investigated previously by several groups.[15−19] The advantage of this process over the widely applied fixed-bed process is well recognized as promoting the gas−solid mixing. We have noted that in general these processes involved the loading of the catalyst/support particles into the bed prior to heating the furnace. The present study demonstrates that a catalyst/support system which is inactive under the fixed-bed synthesis conditions can be activated by simply applying a rapid heating procedure and thus inducing SWNT growth. This dynamic catalyst addition process can also be favorably adapted for continuous production of nanotubes on a commercial basis.

3.2. Effects of Catalyst Loading. Experiments were conducted using the hot-injection synthesis to optimize the growth of SWNTs by using nickel loadings of 0.2, 2.3, 3.0, 3.5, 5.0, 10, 20, and 30 wt % and reaction conditions of $CH_4/Ar = 1$ at 860 °C. In this series of catalysts, SWNTs were obtained from the 2.3, 3.5, and 5.0 wt % nickel loaded catalysts. Figure 5 shows the typical SEM micrographs of the reacted 2.3 wt % nickel loaded catalysts, with 20 nm diameter, fibrous materials distributed uniformly on the surface of the silica gel particles. Raman analysis revealed the presence of RBMs at 180 and 266 cm^{-1} (Figure 3b), which correspond to SWNT diameters of approximately 1.35 and 0.91 nm, respectively, but cannot be interpreted as indicating that these are the only SWNT diameters present. Nevertheless, we note that these tube diameters are similar to those produced from the nickel nitrate/silica gel catalyst system used previously.[20] (The same incident laser was used for both Raman analyses.) This similarity may suggest that the process is controlled by the identity of metal catalyst and substrate regardless of the particular metal catalyst precursor used.

Figure 6 shows the surfaces of the reacted silica gel particles with different nickel loadings. With the lowest nickel loaded catalysts (0.2 wt %), very few nanotubes were observed in the product, although the catalyst powder turned completely black after the synthesis. Raman analysis of the products showed that only poorly crystallized carbon or amorphous carbon was formed under these conditions. This result indicates that the 0.2 wt % nickel loading was too low for efficiently creating the necessary nanosize nickel particles on the surfaces of silica gel particles. At a much higher nickel loading (>10 wt %), the products produced consisted of mainly carbon particles with a mean diameter of 150 nm. Obviously in these cases, large nickel particles were generated during the thermal decomposition due to the high density of nickel precursor. In comparison, the 3.0 wt % nickel loading products, which are within the optimal nickel loading found for SWNT growth, showed a high density of nanotubes on the particle surfaces.

(15) Liu, C.; Liang, Q.; Tang, S. H.; Gao, L. Z.; Zhang, B. L.; Qu, M. Z.; Yu, Z. L. *Chin. Chem. Lett.* **2000**, *11*, 1031.
(16) Venegoni, D.; Serp P.; Feurer, R.; Kihn, Y.; Vahlas, C.; Kalck, P. *Carbon* **2002**, *40* 1799.
(17) Wang, Y.; Wei, F.; Gu, G.; Yu, H. *Physica B* **2002**, *323*, 327.
(18) Qian, W.; Wei, F.; Wang, Z.; Liu, T.; Yu, H.; Luo, G.; Xiang, L. *AIChE J.* **2003**, *49*, 619.
(19) Wang, Y.; Wei, F.; Luo, G.; Yu, H.; Gu, G. *Chem. Phys. Lett.* **2002**, *364*, 568.
(20) Li, Y.; Kinloch, I. A.; Shaffer, M. S. P.; Windle, A. H.; Geng, J.; Johnson, B. *Chem. Phys. Lett.* **2003**, *384*, 98.

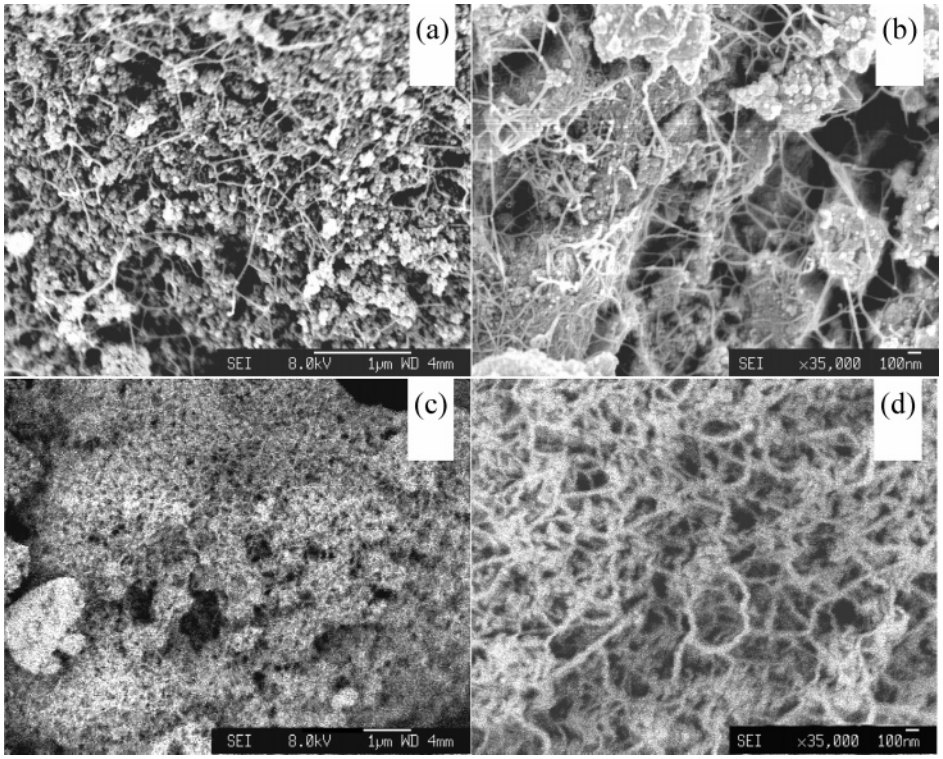

Figure 5. SEM images of the products obtained using 2.3 wt % nickel loaded catalysts at $CH_4/Ar = 1$ and 860 °C. (a) and (b) show the uniform distribution of nanotubes on the silica gel particles, which could be observed on most of the particles in the products. (c) and (d) show particles with densely grown nanotubes, which could be occasionally observed in the products.

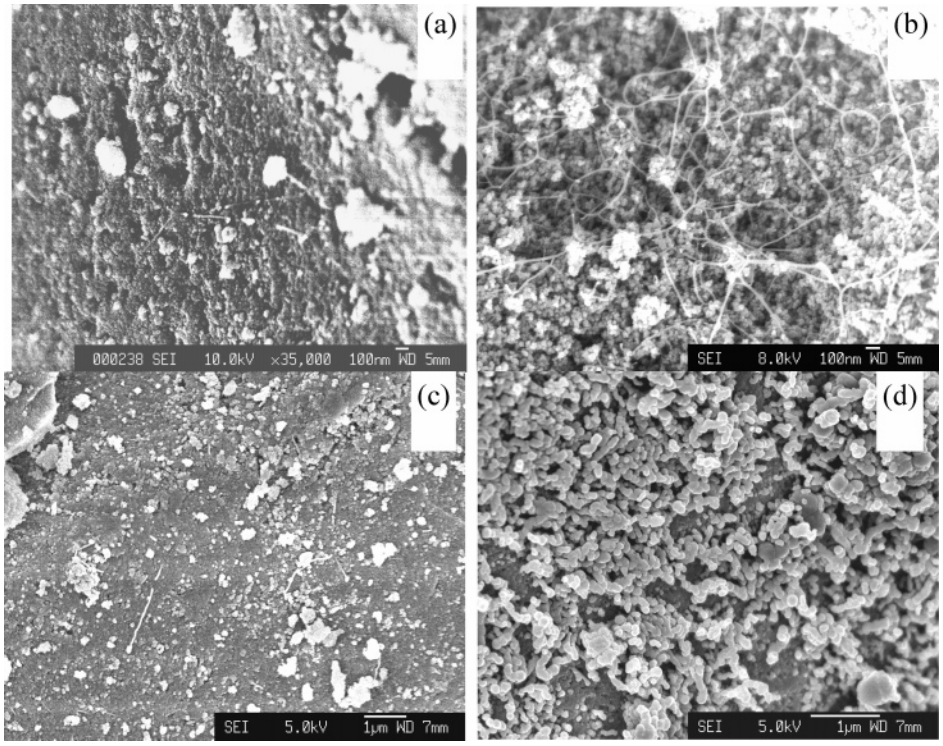

Figure 6. SEM images of the products synthesized using catalysts with nickel loadings of (a) 0.2 wt %, (b) 3.0 wt %, (c) 10 wt %, and (d) 30 wt %. Synthesis conditions: $T = 860$ °C, $CH_4/Ar = 1$, and total flow rate 2.0 L/min.

Although the overall density of the nanotubes observed on the silica gel particles appeared low, careful examination of the nanotube products obtained from 2.3 wt % nickel loaded catalyst found some particles with a dense coverage of carbon nanotubes over the whole surface (Figure 5b,c). This observation shows the potential of this process for high-yield synthesis. Such densely grown nanotubes were obtained previously using a much higher nickel loaded (60 wt %) catalyst with nickel nitrate as the catalyst precursor supported on silica gel particles.[20] However, in the present case, a high nickel loading formate/silica gel catalyst (30 wt %) produced only graphitic particles (Figure 6d). This difference is probably due to the different thermal

decomposition behaviors of the catalyst precursors as they were heated to create the metal catalyst particles on the support substrates. However, the detailed mechanism is not understood yet.

3.3. Effects of Gas Flow Rate and Concentration. The gas flows involved in the synthesis method include the downward carrier gas flow for the initial catalyst injection and the upward flowing reactant gases for subsequent fluidization. The effects of the total flow rate of the methane and argon fluidization gases on the nanotube growth were studied in the range of 0.5−2.4 L/min, with a CH_4/Ar ratio of 1, at a temperature of 860 °C. These gas flow rates were significantly higher than the lower limit of ~0.3 L/min (4.5 cm/s) required for the fluidization of the silica particles at room temperature for $CH_4/Ar = 1$. Since fluidization mainly depends on the mass flow rate, a roughly similar rate through the flow controllers should be suitable when the furnace is heated. However, higher gas flow rates were applied during the synthesis to ensure a complete fluidization of the particles, as their properties change during the growth process. It was found that the growth of SWNTs was virtually independent of the flow rates in the range examined.

The effect of the methane concentration in the gas flow was investigated by comparing CH_4/Ar ratios of 1 and 3 and pure methane, at a synthesis temperature of 860 °C. Results showed that SWNTs could be grown under all these conditions. However, the densities and purities of the nanotubes grown on the surfaces of the silica particles appear to vary with the methane concentration, as observed by SEM observations and Raman spectral analysis (Figures 7 and 8). SEM revealed that the carbon products formed at a CH_4/Ar ratio of unity consisted of clean fibrous materials that are distributed uniformly on the porous surfaces of the support particles, typically crossing between or bridged across small clusters of the catalyst particles (Figure 7a). This result is in agreement with the Raman spectrum (Figure 8a), which shows a much lower D band (1338 cm^{-1}) intensity than G band (1582 cm^{-1}) intensity for $CH_4/Ar = 1$. The ratio of their integrate intensities I_D/I_G is determined to be 0.08, indicating a high purity of nanotubes under these conditions. In contrast, at the higher methane concentration ($CH_4/Ar = 3$), the observable fibrous products on the particle surface were much less, and the filaments appear to be buried partially by an amorphous carbon film on the silica gel particles (Figure 7b). Raman analysis (Figure 7b) showed the D/G ratio ($I_D/I_G = 0.5$) is significantly higher than that at $CH_4/At = 1$ ($I_D/I_G = 0.08$), providing evidence that more amorphous carbon is formed at the high methane concentrations. Furthermore, when pure methane was used, only a few tubes could be observed on the surface of the silica gel particles, which was covered heavily by amorphous carbon (Figure 7c). The Raman spectrum shows the appearance of a very weak RBM band at 263 cm^{-1} but a strong D band ($I_D/I_G = 1.9$). This indicates that pure methane produces mainly amorphous carbon due to the high deposition rate of carbon from the vapor phase.

In the hot-injection synthesis we found that the gaseous environment in the furnace during the hot injection had an important effect on the growth of SWNTs. The upward methane flow through the bed during injection was necessary for the growth of SWNTs. If the injection phase was carried out in the absence of methane, its subsequent introduction into the fluidizing gas did not lead to nanotube production. These results strongly suggest that the activity of the catalyst metal particles survives for only a very short time after their formation, and that, in the absence of hydrocarbon feedstock, the nickel particles quickly agglomerate, deactivating their catalytic properties. For this reason, a mixture of methane and argon was used ($CH_4/Ar = 1$ and a total flow rate of 0.6−1.2 L/min) for injecting the catalyst to provide an immediate carbon source for nanosized nickel particles, which was found to assist the growth of SWNTs. The total flow rate of the carrier

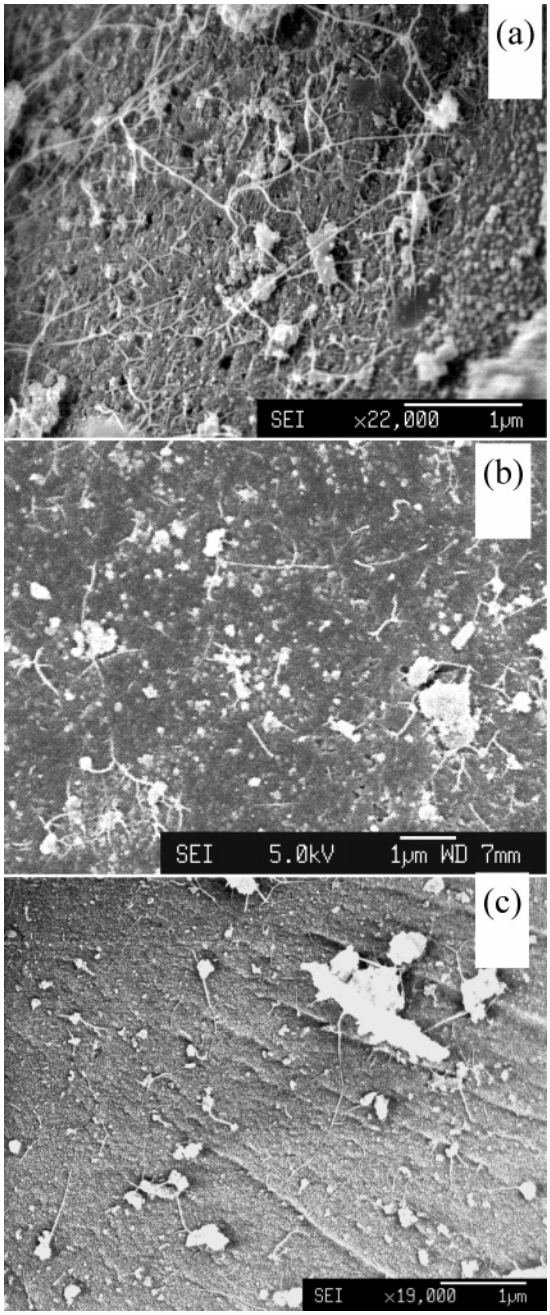

Figure 7. SEM images of the products synthesized at different CH_4/Ar ratios: (a) $CH_4/Ar = 1$; (b) $CH_4/Ar = 3$; (c) pure CH_4, all at $T = 860$ °C using catalysts with a nickel loading of 3.5 wt %.

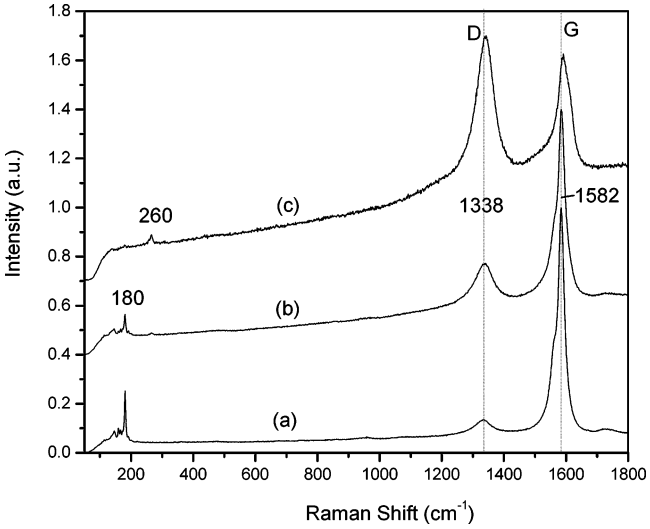

Figure 8. Raman spectra of the products synthesized at different CH_4/Ar ratios: (a) CH_4/Ar = 1; (b) CH_4/Ar = 3; (c) pure CH_4, all at T = 860 °C using catalysts with a nickel loading of 3.5 wt %.

gas was also varied between 0.6 and 1.2 L/min, with no discernible influence on the carbon products being observed.

The rapid injection of the catalyst powders using the cold flow into the hot stream caused some of the catalyst powder to be swept out from the furnace. Characterization of this part of the product provided valuable information on the growth mechanism of the SWNTs. During the injection, an apparently instantaneous color change from light green to black was noticed for these particles, while Raman spectral analysis and SEM analyses showed that SWNTs had already grown on the surfaces on these particles. This result indicates that the growth of SWNTs started almost concurrently with the decomposition of the catalyst precursor to produce the catalyst particles. The residence time for the swept-out particles was estimated to be 40 s, implying that the SWNTs were grown within this period of time. However, SEM showed that the density of the nanotubes on the particles collected from the reactor base was much less than on those collected inside the reactor, indicating that significant growth of the nanotubes occurred during the following fluidization.

4. Conclusions

Single-walled carbon nanotubes were synthesized using a nickel formate precursor on a silica gel support by the fluidized-bed process. The growth of SWNTs was initiated by the rapid injection of the catalyst precursor into the preheated furnace, providing the small catalyst particles required. Without such a hot-injection procedure, no SWNTs were formed; instead, only amorphous carbon was observed. For the hot-injection synthesis, the highest yield of SWNTs was obtained using a nickel loading of 2.4−5.0 wt % on the silica support, while low (<0.2 wt %) and high (>10 wt %) nickel loadings generated amorphous carbon and carbon particles, respectively. The nucleation of SWNTs was found to be sensitive to the gas environment, which needs the presence of hydrocarbon during the thermal decomposition because the small nickel particles only remain active for a short period of time. Finally, the purity and density of the nanotubes were affected by the hydrocarbon concentrations in the gas flow, with lower hydrocarbon concentrations proving optimal.

Acknowledgment. The work was funded by Thomas Swan and Co. Ltd., Consett, County Durham, U.K.

CM0495111